Int. J. Electrochem. Sci., 10 **(2015)** 815 - 822

International Journal of
ELECTROCHEMICAL
SCIENCE
www.electrochemsci.org

Cellular Automata Modeling on Corrosion of Metal with Line Defects

Haitao Wang[*], *En-Hou Han*

Key Laboratory of Nuclear Materials and Safety Assessment, Institute of Metal Research, Chinese Academy of Sciences, Shenyang, 110016, China
[*]E-mail: htwang@imr.ac.cn

Received: 22 October 2014 / *Accepted:* 24 November 2014 / *Published:* 2 December 2014

The formation mechanism of corrosion films on a metal surface with the line defects is studied using a cellular automata approach. To represent the line defects in the model, the regularly spaced columns of metal sites are introduced. These columns are characterized by a corrosion probability higher than that of bulk metal sites. The results show that the influence of defect density on corrosion and film growth can be divided into two stages, and the transition value for the defect density is given. The structural evolution of the film is also investigated by the diffusing species distribution.

Keywords: cellular automata; corrosion; film growth; diffusion; line defects

1. INTRODUCTION

Corrosion is the deterioration a metal undergoes as a result of its interaction with its surroundings. Corrosion not only influences the chemical properties of the metal but also generates changes in its physical properties and its mechanical behavior. The corrosion process is usually electrochemical in nature. A lot of chemical and physical processes take place at the interface between the metal substrate and the ionic solution containing species that can oxidize the metal [1-3]. The corrosion of the metal substrate may give rise to the formation of corrosion films that is insoluble [4,5]. Such films can determine the properties of the metal.

During the last two decades, a large number of literatures concerning the simulations of the formation of films using different simulation methods have been reported [6-8]. Among these simulation methods, the cellular automata model showed the superiority of the recurrence of the real physical systems [9,10]. Taleb and Saunier et al [11-13] used a cellular automata model to describe the role of diffusion and reaction processes in the formation of films on a perfect metal surface. The results

showed that the corrosion front becomes flat and loses the fractal character in the model without the feedback effect. The apparent corrosion rate is greatly reduced compared to the initial corrosion rate by the diffusion. The diffusing species distribution presents particular features as the existence of a fixed concentration at the initial metal/solution plane position. We have studied the diffusion characteristics in the corrosion film on a perfect metal surface by a cellular automata model. The results showed that the diffusing species distribution is the time dependence over the corrosion film. But there exists a diffusing plane in the corrosion film, where the diffusing species concentration does not depend on time. The diffusion steps are found to have great influence on the position and species concentration of the diffusing plane [14].

However, most metals are not perfect. The regular pattern of atomic arrangement is interrupted by the crystal defects, such as point defects, line defects, planar defects [15]. The surface atoms adjacent to the crystal defects have a higher probability of reaction than others because the bonding energy is reduced [16]. So the crystal defects serve as preferential surface sites for corrosion nucleation and propagation [17]. In this work, we use a cellular automata model to study the formation of corrosion films on a metal surface with the line defects.

2. CELLULAR AUTOMATA APPROACH

We want to simulate the following mechanisms. A piece of metal is corroded in contact with the aggressive environment. A part of the corroded species is involved in the formation of the corrosion product that precipitates at the place where the corrosion takes place while the remaining part of the corroded species starts to diffuse across the film. It diffuses until it reaches the growth front where it precipitates as a corrosion product. The transport of the solution species across the film is fast enough not to be explicitly taken into account.

The cellular automata approach is performed on a two-dimensional lattice using four neighbors' rule proposed by Neumann. These four neighbors adjacent to one site refer to upper, down, left and right sites. A rectangular box is used in the simulations. The coordinates of a site (x,y) consist of two integers, x refers to the column and y to the line. The total number of columns and lines is, respectively, N_x and N_y. To represent the line defects in the metal, we introduce regularly spaced columns of metal sites. These columns are characterized by a corrosion probability higher than that of bulk metal sites because the metal atoms located on a defect are in higher energy states. The number of columns introduced divided by the total number of columns is the defect density L_d.

The state of each lattice is determined by the dominating species located at this site. There are five different kinds of species involved in the processes: S, M, M_d, F, D. S denotes the solution species, M denotes the bulk metal species, M_d denotes the metal species located on a line defect, F denotes the corrosion product species, D is the diffusing species. An M or M_d site in contact with at least one F site is called a reactive site for the corrosion. Only this kind of M or M_d site can be transformed. Similarly, an S site in contact with at least one F site is defined as a growth site. The formation of corrosion product involves a volume excess that is due to its stoichiometry, so the corrosion product occupying in a metal site needs not be formed from the equivalent metal species. It

is supposed that the volume excess can be redistributed by the diffusing species D. ω denotes the number of diffusing species formed when an M or M_d is corroded during each time interval, which represents a steric factor related to Pilling-Bedworth ratio [11].

In what follows, two cases are considered: ω=1 and ω=2. When ω=1 the corroded site is replaced by an F site and a new D species is placed in it. When ω=2 one of the two new D species is located on the F site just created and the other is put on one of its nearest neighbor F sites free of D species. If such a site is not found, the corrosion can not occur. In this way, we take into account a feedback effect of the film in formation onto the reaction rate. The effective corrosion probability depends thus on the neighbor of the site. A random walk is used to describe the diffusion process [9]. During each time interval, all the D species try to execute N_D steps. One of four nearest neighbors of a D species is randomly selected. If the selected neighbor is an F site free of D species, the D species moves to it, otherwise the D species stays at its initial position and randomly changes its direction. If the nearest neighbor is an S site, the D species moves to it and it is immediately transformed into an F site.

In the simulations, the periodic boundary conditions are applied in the x direction. The total number of columns N_x and lines N_y is, respectively, 1000 and 1000. At the initial time, the lines up to y=499 are filled with the solution sites. The line y=500 is formed of the film. The lattices are filled up with the bulk metal sites or the metal sites located on the line defects starting from the line y=501. The lattice spacing α is considered as the unit of length and the interval of simulation time τ is taken as 1.

3. RESULTS AND DISCUSSION

3.1 The corrosion current

Figure 1 shows the corrosion current I as a function of the simulation time N_t at different defect density L_d. Here, the results correspond to the corrosion probability for the bulk metal P=0. 05, the corrosion probability for the metal located on the line defect P_d=0.1, the diffusion steps N_D=100. The corrosion current I is given by $I = N_{corr} / \tau$, in which N_{corr} is the number of corroded metal. As shown in Figure 1a, for ω=1, a strong increase of corrosion current at the beginning of the process is observed, then the corrosion current reaches a plateau value after $N_t \approx 200$. The corrosion current increases as the defect density increases. The corrosion current is determined by the corrosion probability and the number of active corrosion sites. It can be seen in Figure 2a that the active corrosion sites ratio r_a (the number of active corrosion sites N_a divided by the number of initial active corrosion sites N_m) for different defect density doesn't have great changes. The value of r_a is about 2 for L_d=0 and L_d=1, and $r_a \approx 2.3$ for others L_d. So for given corrosion probability P and P_d, the larger is the defect density, the larger is the corrosion current in the case of ω=1. Figure 1b shows that for ω=2, the corrosion current increases quickly with the increasing of the simulation time, then decreases very slowly for longer times. The active corrosion sites have the similar behavior in Figure 2b. The corrosion current fluctuates in the wide range for all defect density, which is expected since the feedback effect occurs.

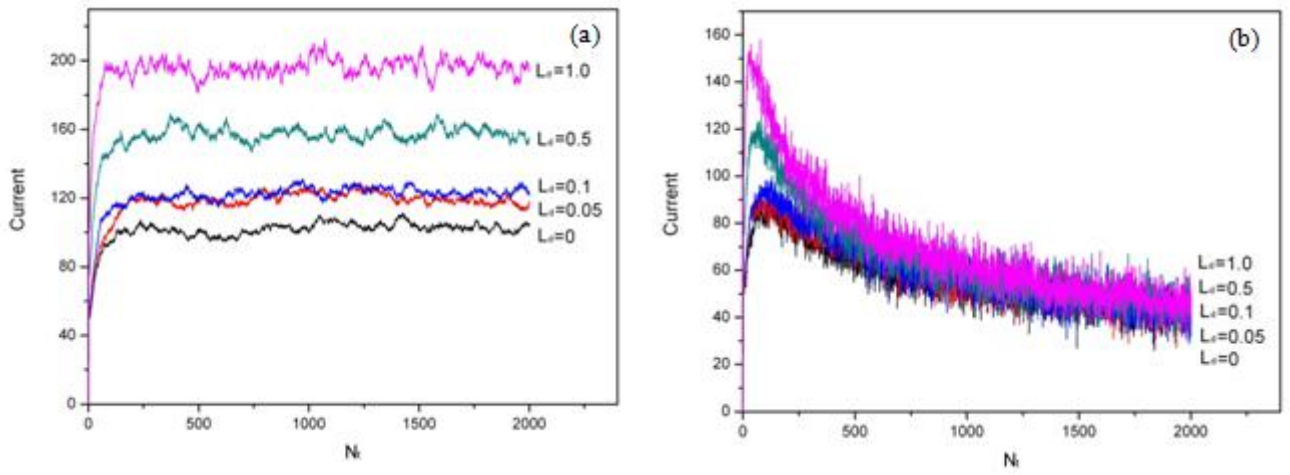

Figure 1. The corrosion current as a function of the simulation time for (a) ω=1 and (b) ω=2 when P=0. 05, P_d=0.1, N_D=100

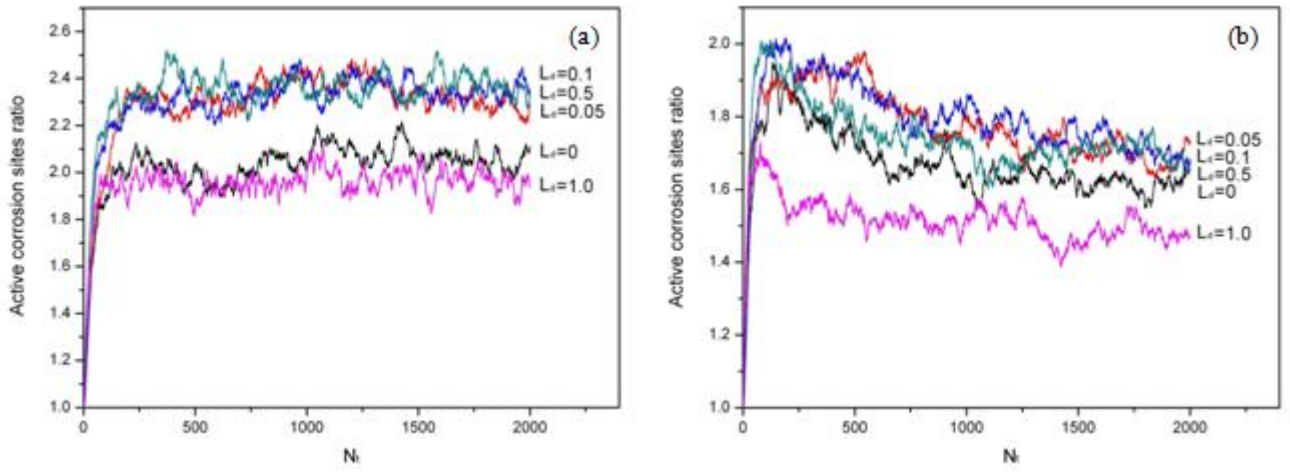

Figure 2. The active corrosion sites ratio as a function of the simulation time for (a) ω=1 and (b) ω=2 when P=0. 05, P_d=0.1, N_D=100

3.2 The evolution of the corrosion and the film growth

The corrosion depth ratio and the film thickness ratio as a function of the defect density are shown in Figure 3. The corrosion depth ratio r_c and the film thickness ratio r_f are defined as:

$$r_c = \frac{\overline{h_c}}{h_m} \qquad \overline{h_c} = \frac{1}{N_x}\sum_{x=1,N_x} h_c(x) - h_0 \qquad (1)$$

$$r_f = \frac{\overline{h_f}}{h_m} \qquad \overline{h_f} = h_0 - \frac{1}{N_x}\sum_{x=1,N_x} h_f(x) \qquad (2)$$

Where $\overline{h_c}$ and $\overline{h_f}$ are, respectively, the corrosion depth and the film thickness. $h_c(x)$and $h_f(x)$ are, respectively, for the column x the highest value of the line y for which there is a metal site and a

corrosion product site. h_0 is the initial position of the metal/solution plane interface, h_m is the initial metal thickness.

Figure 3a shows that whatever the value of steric factor ω, the influence of defect density on corrosion depth ratio can be divided into two stages. The curve obeys a power law at the initial time, however, with the increasing of the defect density the linear relation is observed. The transition value for the defect density is about 0.1. The corrosion depth for ω=1 is much larger than that at ω=2, and the value of r_c is 0.49 when L_d=0.1 for ω=1, whereas r_c=0.24 for ω=2. The increasing rate of the corrosion depth for ω=1 is much quicker than that at ω=2. For ω=1, when the metal is perfect (L_d=0), the corrosion depth ratio is given by $r_c = PN_aN_t / N_xh_m$. The corrosion depth ratio corresponding to the limit L_d=1 is given by $r_c = P_dN_aN_t / N_xh_m$. Therefore, the defect density can significantly promote the corrosion depth. For ω=2, the corrosion rate depends on not only the corrosion probability but also the diffusion rate. The diffusion must bring on at least an F site free of D species for the corrosion site, which reduces the corrosion rate, so the corrosion depth for ω=2 is much lower than that at ω=1.

Figure 3b shows that the film thickness increases with the increasing of the defect density. The influence of defect density on film thickness follows the same law as that of corrosion depth. The transition value for the defect density is also about 0.1. The film thickness is much larger in the case of ω=2 than in the case of ω=1, and the increasing rate of the film thickness has the same value for ω=1 and ω=2. The film growth is caused by the diffusion and the deposition of D species across the film. For ω=2, the diffusion process is more efficiency, which promotes the film growth. We will give more consideration to this reason in next section.

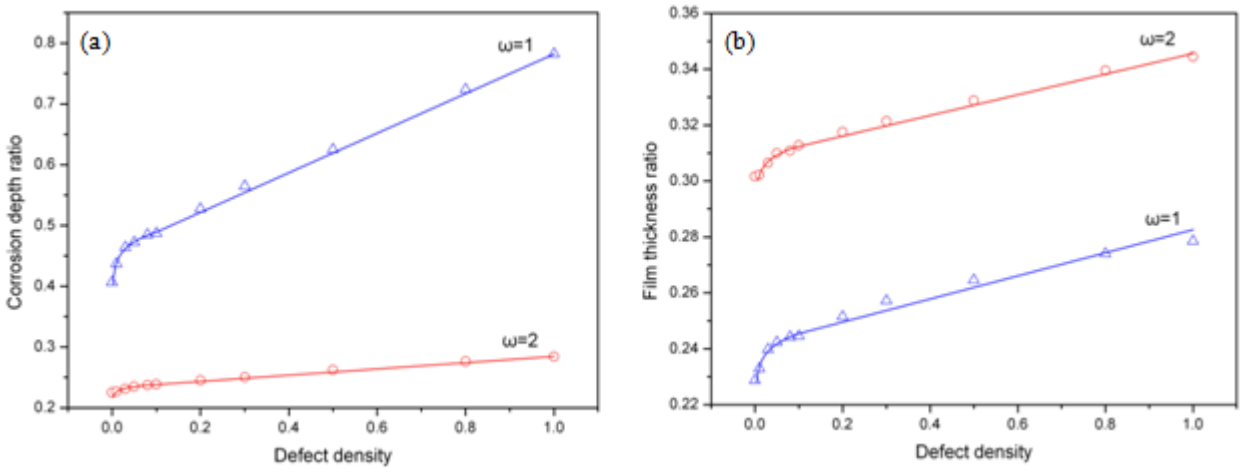

Figure 3. The corrosion depth ratio (a) and the film thickness ratio (b) as a function of the defect density for P=0. 05, P_d=0.1, N_D=100, N_t=2000

3.3 The diffusing species distribution

Figure 4 shows the diffusing species concentration as a function of the line y position at given values of N_t. It can be seen that the diffusing species distribution has a form of a triangular peak for ω=1 and ω=2. The diffusing species concentration begins at the growth front, and increases by a linear

dependence. Near the corrosion front, it reaches a highest concentration and decreases rapidly to vanish at the corrosion front. The thickness of this narrow region corresponds to the roughness of the corrosion front. It is clearly visible that for ω=1, the advancement of the growth front is slower than that at ω=2 and the advancement of the corrosion front is faster than that at ω=2, which agrees with the results in Figure 3a and Figure 3b. The maximum concentration near the corrosion front for ω=1 is larger than that in the case of ω=2 at the same simulation time because of the feedback effect. It can be found from the area under the distributions that for ω=2, the total number of D species is reduced by the feedback effect although the number of D species inserted is two times more than in the case of ω=1 during each time interval, and the gradient of the D species concentration is higher in the case of ω=2. These phenomena suggest that the diffusion process is more efficiency in the case of ω=2.

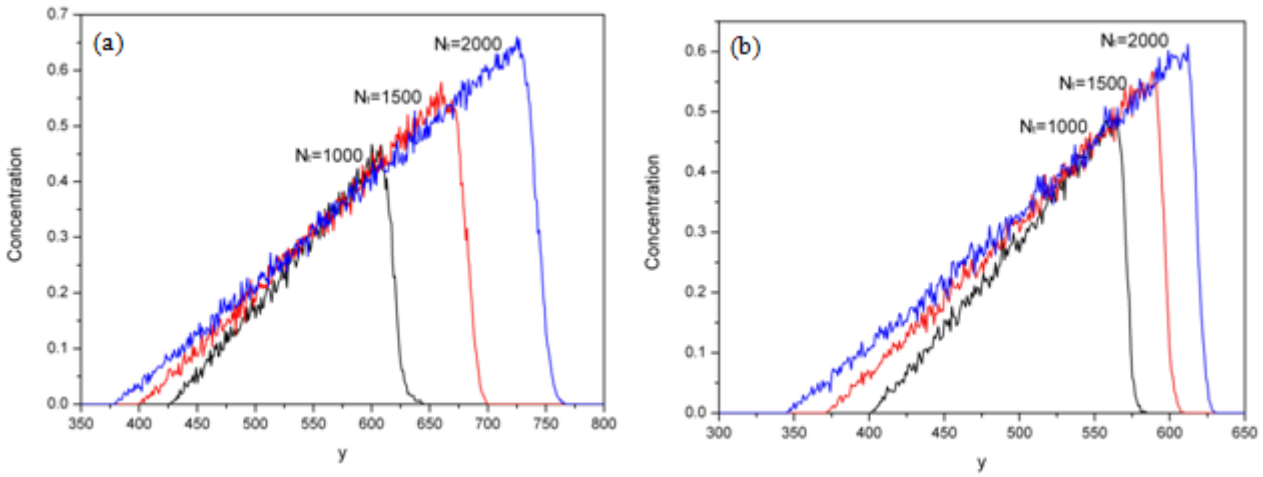

Figure 4. The diffusing species concentration as a function of the line y position for (a) ω=1 and (b) ω=2 when P=0. 05, P_d=0.1, L_d=0.1, N_D=100

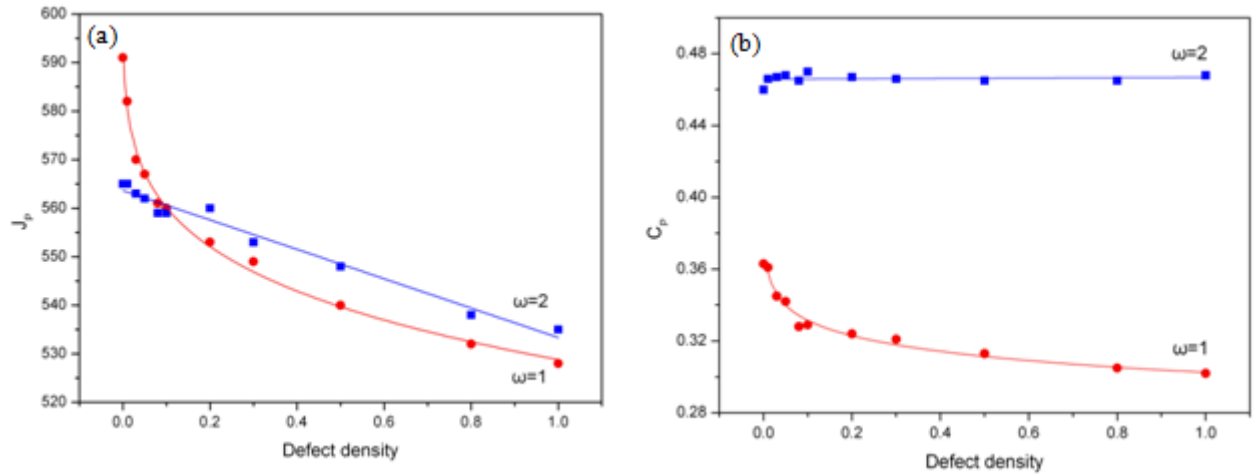

Figure 5. (a) The plane position J_p and (b) the plane concentration C_p as a function of the defect density for P=0. 05, P_d=0.1, N_D=100

It can be observed in Figure 4 that all the profiles have only one common intersection point. It suggests that there exists a plane in the film where the diffusing species concentration remains constant. The plane position J_P is about 560, and the plane concentration C_P is about 0.33 for ω=1. The plane position J_P is about 559, and the plane concentration C_P is about 0.47 for ω=2. The plane position J_p and the plane concentration C_p as a function of the defect density is shown in Figure 5. The plane position J_P decreases as the defect density increases. The plane position J_P follows the power law $J_P = 617.89 - 89.10L_d^{0.19}$ for ω=1, while the plane position J_P follows the linear law $J_P = 563.63 - 30.30L_d$ for ω=2. The plane concentration C_p has the same form as the plane position J_P, $C_P = 0.72 - 0.42L_d^{0.03}$ when ω=1, and $C_P = 0.47$ when ω=2.

3.4 Mapping between cellular automata model and experiment data

A mapping between cellular automata simulation and experimental data is performed in order to understand more clearly the mesoscopic modeling of the corrosion of the metal with the line defects. When the corrosion happens, the time interval τ represents the time needed to destroy a piece of metal and to form a cluster of F species at a distance δ. Therefore the corrosion rate is given by:

$$\nu = P\delta / \tau \qquad (3)$$

To the corrosion of carbon steels and low alloy steels in the seawater as an example, the average corrosion rate is usually 0.1mm/a. In order to simplify the computation process, only the pure defect with L_d=1 is considered in this mapping. Supposed that the corrosion probability P_d is 0.1, and the lattice constant δ is 10nm, so the time interval τ can be calculated to be 5.3min. Based on the simulation data at ω=1 in Figure 3, the corrosion depth and the film thickness are approximately 3.9μm and 1.4μm respectively after 177h.

4. CONCLUSIONS

The cellular automata model is used to simulate the film formation on a metal surface with the line defects. In the simulation, the corrosion current for ω=1 increases when the defect density increases. The corrosion current for ω=2 fluctuates in the wide range for all defect density because the feedback effect happens. Whatever the value of ω, the effect of defect density on corrosion depth and film thickness can be divided into two stages. The curve follows a power law at the initial time, however, with the increasing of the defect density the linear relation is obtained. The transition value for the defect density is about 0.1. It is observed from the diffusing species distribution that the total number of D species for ω=2 is less than that at ω=1, and the gradient of the D species concentration is higher in the case of ω=2. The plane position J_p and the plane concentration C_p have a power function of the defect density for ω=1, while follow a linear law in the case of ω=2.

ACKNOWLEDGEMENTS
This work is supported by the National Science and Technology Major Project (No. 2011ZX06004-009).

References

1. A. Cox and S. B. Lyon, *Corros. Sci.*, 36 (1994) 1177
2. Z. Pilbath and L. Sziraki, *Electrochim. Acta*, 53 (2008) 3218
3. N. Birbilis, M. K. Cavanaugh and R. G. Buchheit, *Corros. Sci.*, 48 (2006) 4202
4. P. Volovitch, C. Allely and K. Ogle, *Corros. Sci.*, 51 (2009) 1251
5. S. Q. Zheng, L. W. Liu, C. S. Zhou, L. Q. Chen and C. F. Chen, *Int. J. Electrochem. Sci.*, 8 (2012) 1434
6. A. L. Barabasi and H. E. Stanley, *Fractal Concepts in Surface Growth*, Cambridge University Press, Cambridge (1995)
7. E. Somfai, R. C. Ball, N. E. Bowler and L. M. Sander, *Physica A*, 325 (2003) 19
8. I. Nainville, A. Lemarchand and J. P. Badiali, *Electrochim. Acta*, 41 (1996) 1855
9. B. Chopard and M. Droz, *Cellular Automata Modeling of Physical Systems*, Cambridge University Press, Cambridge (1998)
10. H. T. Wang and E. -H. Han, *Electrochim. Acta*, 90 (2013) 128
11. A. Taleb, A. Chausse, M. Dymitrowska, J. Stafiej and J. P. Badiali, *J. Phys. Chem. B*, 108 (2004) 952
12. J. Saunier, M. Dymitrowska, A. Chausse, J. Stafiej and J. P. Badiali, *J. Electroanal. Chem.*, 582 (2005) 267
13. J. Saunier, A. Chausse J. Stafiej and J. P. Badiali, *J. Electroanal. Chem.*, 563 (2004) 239
14. H. T. Wang and E. -H. Han, *J. Mater. Sci. Technol.*, 28(2012) 427
15. A. Kelly, G. W. Groves and P. Kidd, *Crystallography and Crystal Defects*, John Wiley & Sons, Inc., New York (2000)
16. R. S. Lillard, G. F. Wang and M. I. Baskes, *J. Electrochem. Soc.*, 153 (2006) B358
17. A. Taleb, J. Stafiej and J. P. Badiali, *J. Phys. Chem. C*, 111 (2007)